STAT1 accelerates cutaneous melanoma progression through TUBB4A expression regulation

RONGXIN ZHAO[1], KEXIN FANG[2], XIAOFEI ZHANG[3] and HONGCHAO LI[4]

[1]Department of Dermatology, Pudong New Area People's Hospital, Shanghai 201200; P.R. China; [2]Department of Dermatology, 921st Hospital of Joint Logistics Support Force People's Liberation Army of China, The Second Affiliated Hospital of Hunan Normal University, Changsha, Hunan 410073, P.R. China; [3]Shanghai Xinmei Medical Beauty Outpatient Department, Shanghai 200031, P.R. China; [4]Department of Head and Neck Surgery, The Second Hospital of Zhuzhou City, Zhuzhou, Hunan 412000, P.R. China

Received October 9, 2025; Accepted January 22, 2026

DOI: 10.3892/mmr.2026.13828

Abstract. The present research explored the contributions of signal transducer and activator of transcription 1 (STAT1) and tubulin β4A (TUBB4A) in melanoma pathogenesis, focusing on their roles in modulating cellular proliferation, motility and apoptotic pathways. The goal of the study was to establish foundational evidence of the role of these proteins in melanoma for the development of precision therapeutic interventions. Gene silencing approaches were utilized to suppress STAT1 expression, while TUBB4A overexpression was achieved both *in vitro* and in a murine xenograft model. Cellular proliferation was evaluated via Cell Counting Kit-8 and colony formation assay, whereas migration capacity was assessed using Transwell migration assays. Apoptotic activity was quantified by flow cytometry using Annexin V-FITC and PI staining. Western blot analysis was performed to measure the protein expression levels of STAT1 and TUBB4A. STAT1 downregulation led to impaired proliferation and motility in A375 and RPMI-7951 melanoma cell lines, concomitant with increased apoptotic rates. These phenotypic changes were partially reversed following TUBB4A overexpression. *In vivo* experiments demonstrated significantly smaller tumor volumes in STAT1 knockdown xenografts, although TUBB4A overexpression partially restored neoplastic growth. STAT1 drove melanoma progression by upregulating TUBB4A, which acted as a downstream signaling mediator. The ability of TUBB4A to counteract STAT1 inhibition effects suggested that targeting this regulatory axis represents a potential therapeutic strategy. The findings of the present study contributed novel mechanistic insights that may facilitate the development of innovative melanoma treatment modalities.

Correspondence to: Professor Hongchao Li, Department of Head and Neck Surgery, The Second Hospital of Zhuzhou City, 269 Xiangtian East Road, Shifeng, Zhuzhou, Hunan 412000, P.R. China
E-mail: hongchao808@163.com

Abbreviations: CCK-8, Cell Counting Kit-8; ChIP, chromatin immunoprecipitation; DFS, disease-free survival; FBS, fetal bovine serum; GEPIA, Gene Expression Profiling Interactive Analysis; HEM, human epidermal melanocytes; HR, hazard ratio; JAK, Janus kinase; OS, overall survival; Ov-NC, negative control lentiviral overexpression vector; Ov-TUBB4A, lentiviral vector for tubulin β4A overexpression; PBS, phosphate-buffered saline; si-NC, negative control small interfering RNA; si-STAT1, small interfering RNA targeting signal transducer and activator of transcription 1; SKCM, skin cutaneous melanoma; STAT1, signal transducer and activator of transcription 1; STAT3, signal transducer and activator of transcription 3; TPM, transcripts per million; TUBB4A, tubulin β4A

Key words: STAT1, cutaneous melanoma, TUBB4A, apoptosis, migration

Introduction

Skin cutaneous melanoma (SKCM) is a malignant form of skin cancer with an increasing incidence and mortality rate, presenting notable challenges to patient health and survival (1). Despite the progress made in targeted therapies and immunotherapy against SKCM, numerous patients develop resistance or exhibit only partial responses, resulting in suboptimal therapeutic outcomes (2). Consequently, further investigation into the molecular mechanisms driving melanoma progression is required. Identifying novel therapeutic targets and reliable biomarkers for SKCM is important for improving treatment strategies and patient prognosis.

Signal transducer and activator of transcription (STAT)1, a central component of the Janus kinase (JAK)-STAT signaling pathway, regulates the expression of numerous downstream genes involved in important cellular functions, including proliferation, differentiation, apoptosis and immune response modulation (3,4). In the context of cancer, STAT1 is often described as a double-edged sword, exhibiting both tumor-suppressing and tumor-promoting properties. For example, in breast and colorectal cancers, STAT1 generally acts as a tumor suppressor by inducing apoptosis and enhancing immune responses to limit tumor progression (5). Clinical evidence suggests that STAT1 expression is markedly elevated in melanoma tissues compared with healthy skin, with this upregulation associated with poor clinical outcomes (6). In line with these observations, an *in vitro* study showed

that silencing STAT1 reduces melanoma cell proliferation and migration while promoting apoptosis, underscoring its oncogenic role in melanoma (7). However, the downstream molecular mechanisms regulated by STAT1 remain to be fully elucidated, and the incompletely resolved interactions of STAT1 with other notable molecular targets warrant further exploration.

Tubulin β4A (TUBB4A), a member of the tubulin β-chain family, encodes β-tubulin, a notable protein involved in maintaining cellular integrity and supporting important cellular processes such as cell division and migration (8). Elevated expression of TUBB4A has been reported in various cancers, including glioblastoma, breast cancer and lung cancer, with its upregulation being associated with enhanced tumor invasiveness and resistance to therapeutic interventions (9,10). However, the precise role of TUBB4A and its regulatory mechanisms in melanoma remain largely unexplored. The JAK-STAT signaling pathway is important for tumor initiation and progression, with STAT1 and STAT3 acting as central regulators of downstream gene expression. These factors modulate important cellular processes in cancer, including proliferation, apoptosis and immune evasion (11-13). In melanoma, aberrant STAT1 activation may interact with molecules such as TUBB4A, thereby enhancing tumor invasiveness and conferring resistance to chemotherapy (14,15). As a well-established oncogene, STAT3 promotes tumor growth and metastasis by modulating cytokine expression and interacting with other transcription factors (16,17). The interplay between STAT1 and STAT3 in melanoma is multifaceted, characterized by both synergistic and antagonistic interactions that necessitate further investigation (6,18,19).

Although TUBB4A upregulation has been implicated in tumor progression and poor prognosis across various cancers, its exact role in melanoma remains poorly defined. Evidence suggests that TUBB4A is important for maintaining microtubule stability, a function necessary for processes such as tumor cell mitosis (20,21), migration (22) and invasion (10). Furthermore, TUBB4A appears to contribute to chemotherapy resistance, with its elevated expression linked to drug resistance in cancers, including breast cancer and non-small cell lung cancer, particularly to agents such as paclitaxel (23,24). Similar mechanisms may be at play in melanoma, although tumor-specific factors are likely to influence these processes. Understanding how STAT1 influences TUBB4A expression is important for elucidating melanoma pathogenesis and identifying potential therapeutic targets for SKCM.

The present study aimed to assess the roles of STAT1 and TUBB4A in melanoma cell proliferation, migration and apoptosis, using both *in vitro* and *in vivo* models. Additionally, the impact of these molecules on tumor growth were evaluated in a mouse xenograft model, providing a comprehensive analysis of the functional and mechanistic contributions of the STAT1-TUBB4A pathway to melanoma. With the increasing use of targeted therapies and immunotherapies (25,26), the discovery of novel biomarkers and treatment strategies for SKCM is important for improving patient outcomes. The present research endeavored to clarify the STAT1-TUBB4A axis, laying the groundwork for the development of more personalized and effective therapeutic approaches for patients with melanoma.

Materials and methods

Bioinformatics analysis. RNA sequencing data for TUBB4A and STAT1 expression across various cancer types were obtained from the Gene Expression Profiling Interactive Analysis 2 (GEPIA2) database (http://gepia2.cancer-pku.cn), which processes data from The Cancer Genome Atlas (TCGA) and the Genotype-Tissue Expression (GTEx) project (search term, SKCM | Skin Cutaneous Melanoma). The analysis was conducted in March 2024.

For the specific analysis of SKCM, the TCGA-SKCM tumor dataset (n=461) was compared against the GTEx normal skin tissue dataset (n=558). Differential expression analysis was performed using the following parameters: A $|\log_2$fold change (FC)$|$ cut-off value of 1 and a P-value cut-off value of 0.05. Gene expression levels for TUBB4A and STAT1 were quantified as transcripts per million (TPM).

To identify potential binding sites of the transcription factor STAT1 within the regulatory region of the TUBB4A gene promoter, bioinformatics analysis was performed using the JASPAR database (https://jaspar.elixir.no/). First, the experimentally validated canonical position weight matrix for STAT1 was retrieved from JASPAR, while the promoter sequence spanning approximately from -2,000 bp to + 500 bp relative to the transcription start site of TUBB4A was extracted from a genomic database. Subsequently, the 'Scan' function in JASPAR was used to scan this promoter sequence for STAT1 binding motifs, with a threshold set at an 85% relative score. The analysis finally generated a prediction list containing specific coordinates, match scores, and statistical significance of the identified sites, thereby providing candidate targets for subsequent experimental validation.

Patient samples and clinical data. A total of 31 SKCM tissue samples and matching normal tissue samples were collected from patients at Pudong New Area People's Hospital (Shanghai, China), with institutional review board approval (approval no. CEA-2023-16) and in compliance with ethical guidelines. The patient cohort consisted of 18 males and 13 females, with a median age of 62 years and an age range of 38-75 years. All patients provided informed consent for tissue use. Melanoma samples were obtained from patients undergoing surgical resection of primary tumors, and matching normal tissue was collected from adjacent healthy skin during the same procedure. Specimens were immediately snap-frozen in liquid nitrogen and stored at -80˚C until RNA extraction. Normal tissue was taken at least 2 cm from the tumor to avoid potential contamination.

Cell culture and treatment. The melanoma cell lines A2058 (cat. no. CRL-3601), SK-MEL-1 (cat. no. HTB-67), A375 (cat. no. CRL-1619) and RPMI-7951 (cat. no. HTB-66), as well as normal human epidermal melanocytes (HEM; cat. no. PCS-200-013) and 293T cells (cat. no. CRL-3216) were obtained from American Type Culture Collection. Cells were cultured in DMEM (cat. no. 11995-065; Thermo Fisher Scientific, Inc.) supplemented with 10% fetal bovine serum (FBS; cat. no. 16000-044; Gibco; Thermo Fisher Scientific, Inc.) at 37˚C in a humidified atmosphere containing 5% CO_2. Cells were seeded into 6-well plates and grown to 60-70%

confluence. Transfection was performed using Lipofectamine® 3000 (cat. no. L3000015, Thermo Fisher Scientific, Inc.) according to the manufacturer's protocol. Cells were transfected with small interfering RNA (siRNA) targeting STAT1 (si-STAT1; cat. no. A09009) or a scrambled negative control (si-NC; cat. no. A09010; GenePharma, Shanghai) at a final concentration of 50 nM. The cells were incubated with the transfection complexes at 37˚C for 48 h prior to subsequent experimentation. The sequences of siRNAs are listed in Table SI. Lentiviral Vector Generation and Transduction Stable TUBB4A overexpression was achieved using a lentiviral system. The lentiviral vector encoding the TUBB4A gene (Ov-TUBB4A, pReceiver-Lv105) and the negative control vector lacking the insert (Ov-NC; pReceiver-Lv105 Empty Vector) were purchased from GeneCopoeia, Inc. Lentiviral particles were generated using a 3rd generation packaging system in 293T cells (ATCC). Briefly, HEK293T cells were co-transfected with 2.5 μg of the lentiviral plasmid, along with packaging and envelope plasmids (Lenti-Pac™ HIV Expression Packaging Kit; GeneCopoeia, Inc.) using the EndoFectin™ Lenti transfection reagent (cat. no. EF002; GeneCopoeia, Inc.). The ratio of the target plasmid to the packaging mix was maintained at 1:1. Lentiviral supernatants were collected at 48 and 72 h post-transfection and filtered through a 0.45-μm filter. Melanoma cells were infected with the viral particles at a multiplicity of infection (MOI) of 10 in the presence of 8 μg/ml Polybrene (cat. no. TR-1003; Sigma-Aldrich; Merck KGaA). The transduction duration was 24 h, after which the medium was replaced with fresh complete medium. Selection of stably transfected cells was performed 48 h post-transduction using 2 μg/ml puromycin (cat. no. P9620; Sigma-Aldrich). At 24 h after the transfection, the mRNA levels of STAT1 and TUBB4A were measured using reverse transcription-quantitative (RT-q)PCR.

RT-qPCR. Total RNA was acquired from cellular and tumor specimens through the TRIzol method (Invitrogen; Thermo Fisher Scientific, Inc.). RT-qPCR was performed using a SuperScript™ III Platinum™ One Step RT-qPCR Kit (cat. no. 11732088; Thermo Fisher Scientific, Inc.). The thermocycling conditions were as follows: cDNA synthesis at 50˚C for 15 min; initial denaturation at 95˚C for 2 min, followed by 40 cycles of denaturation at 95˚C for 15 sec and annealing/extension at 60˚C for 30 sec. Relative transcript abundances were determined utilizing the $2^{-\Delta\Delta Cq}$ algorithm (27). The primers were as follows: STAT1: Forward, 5'-GACCGCACCTTC AGTCTTTTC-3' and reverse, 5'-TCATTCACATCTCTCAAC TTCACA-3'; TUBB4A: Forward: 5'-GCTGCGGACCGA GAAACT-3', Reverse: 5'-TCCAGTTGCAGGTCACTGTC-3'; GAPDH: Forward: 5'-CCACTCCTCCACCTTTGAC-3' and reverse: 5'-ACCCTGTTGCTGTAGCCA-3'.

Cell Counting Kit-8 (CCK-8). Cell viability was assessed using a CCK-8 assay (cat. no. CK04; Dojindo Laboratories, Inc.). Following treatment with siRNA or lentiviral vectors, cells were seeded in triplicate into 96-well culture plates (cat. no. 3599; Corning, Inc.) at a density of $5x10^3$ cells/well and allowed to adhere for 24 h. The medium was subsequently replaced with 100 μl of fresh growth DMEM supplemented with FBS as aforementioned and 10 μl of CCK-8 reagent was added to each well. The plates were incubated with CCK-8 reagent at 37˚C for 1-4 h, depending on the cell type, to allow for the conversion of the tetrazolium salt into a formazan product by metabolically active cells. Absorbance was measured at 450 nm using a BioTek 800 TS Absorbance Reader (cat. no. ELx800; BioTek; Agilent Technologies, Inc.).

Colony formation assays. Melanoma cells (A375 and RPMI-7951) were seeded into 6-well plates (cat. no. 3516; Corning, Inc.) at a density of 500-1,000 cells per well and allowed to adhere for 24 h. Cells were then transfected with si-NC (cat. no. A09010) or si-STAT1 (cat. no. A09009; GenePharma), as well as transfected using a lentiviral vector for TUBB4A overexpression (Ov-TUBB4A; pReceiver-Lv105; GeneCopoeia, Inc.) or Ov-NC (pReceiver-Lv105 Empty Vector; GeneCopoeia, Inc.). After 10-14 days incubation, colonies were fixed with 4% paraformaldehyde (cat. no. J19943.K2; Thermo Fisher Scientific, Inc.) for 15 min, stained with 0.5% crystal violet solution (cat. no. C3886; MilliporeSigma; Merck KGaA) for 30 min and washed with phosphate-buffered saline (PBS; cat. no. 10010-023; Thermo Fisher Scientific, Inc.). Colonies, defined as clusters of ≥50 cells, were manually counted under a microscope (Nikon Corporation) at x20 magnification. The results were normalized to the control group.

Flow cytometry for apoptosis assay. Briefly, melanoma cells (A375 and RPMI-7951) were seeded into 6-well plates and treated with siRNA or lentiviral vectors as aforementioned. To induce apoptosis, cells were exposed to 100 nM cisplatin (cat. no. P4394; Sigma-Aldrich) for 24 h at 37˚C. Following treatment, cells were harvested, washed with cold PBS and resuspended in Annexin V binding buffer at a concentration of $1x10^6$ cells/ml. Cells were then stained with 5 μl Annexin V-FITC and 5 μl PI for 15 min at room temperature in the dark. The cell suspension was filtered through a 40-μm nylon mesh to remove large aggregates. Flow cytometric analysis was immediately performed using a BD FACSCalibur™ (BD Biosciences) flow cytometer, and data were processed using FlowJo software (version 10.8.1, BD Biosciences). A sequential gating strategy was employed: The primary cell population was first identified on an forward scatter area vs. side scatter area dot plot while excluding debris. Subsequently, single cells were identified using forward scatter height vs. forward scatter area density plots to exclude doublets and aggregates. Apoptosis analysis was conducted on this gated singlet population. All flow cytometry data were analyzed using a standardized gating strategy with gating parameters maintained consistently across all experimental groups. The proportion of cells in early apoptosis (Annexin V-positive, PI-negative), late apoptosis and necrosis (Annexin V-positive, PI-positive) and live cells (Annexin V-negative, PI-negative) were determined.

Cell migration assay. Cell migration was evaluated using Transwell inserts with 8 μm pore chambers (cat. no. 3422; Corning, Inc.). Cells (A375 and RPMI-7951) were seeded in serum-free DMEM (cat. no. 11995-065; Thermo Fisher Scientific, Inc.) in the upper chamber at a density of $5x10^4$ cells/well, while DMEM supplemented with 10% FBS (cat. no. 16000-044; Gibco; Thermo Fisher Scientific, Inc.)

was used in the lower chamber. After 24 h-incubation at 37˚C, migrated cells were fixed with 4% paraformaldehyde (cat. no. J19943.K2; Thermo Fisher Scientific, Inc.) for 15 min at 25˚C, stained with 0.1% crystal violet solution (cat. no. C3886; MilliporeSigma; Merck KGaA) for 30 min at 25˚C and washed with PBS (cat. no. 10010-023; Thermo Fisher Scientific, Inc.). Migrated cells were visualized under an inverted light microscope (Nikon Corporation) for analysis. The number of migrated cells was quantified using ImageJ software (Version 1.53e, National Institutes of Health).

Western blot analysis. A375 and RPMI-7951 cells were harvested, and proteins were extracted using RIPA buffer (cat. no. 89900; Thermo Fisher Scientific, Inc.) containing protease inhibitors (cat. no. 11836170001; Roche Diagnostics, Ltd.). Protein concentrations were quantified using the Pierce™ BCA Protein Assay Kit (cat. no. 23225; Thermo Fisher Scientific, Inc.). A total of 20 μg protein in each lane was separated by 10% SDS-PAGE and transferred to PVDF membranes (cat. no. IPVH00010; MilliporeSigma; Merck KGaA). Membranes were blocked with 5% non-fat milk (cat. no. 1706404; Bio-Rad Laboratories, Inc.) in TBST with 0.1% Tween 20 for 1 h at 25˚C and incubated overnight at 4˚C with primary antibodies against STAT1 (1:1,000; cat. no. 14994; Cell Signaling Technology, Inc.) and TUBB4A (1:1,000; cat. no. ab11315; Abcam), as well as GAPDH (1:5,000; cat. no. 2118; Cell Signaling Technology, Inc.) serving as a loading control. After washing three times with TBST, membranes were incubated with HRP-conjugated goat anti-rabbit IgG (cat. no. 7074; Cell Signaling Technology, Inc.) and horse anti-mouse IgG (both 1:2,000, cat. no. 7076; Cell Signaling Technology, Inc.) secondary antibodies at room temperature for 1 h. Protein bands were visualized using SuperSignal™ West Pico PLUS Chemiluminescent Substrate (cat. no. 34095; Thermo Fisher Scientific, Inc.). The band intensity was semi-quantified using ImageJ software (version 1.53e, National Institutes of Health).

Luciferase reporter assay. The promoter regions of TUBB4A were cloned into the firefly luciferase reporter plasmid pGL3-Basic vector (cat. no. E1741; Promega Corporation) and transfected into 293T cells. The cells were transiently co-transfected with the reporter constructs, the internal control Renilla luciferase vector (cat. no. E2261; Promega Corporation), and si-STAT1 (cat. no. A09009; GenePharma, Shanghai) as aforementioned. STAT1 knockdown was performed using si-STAT1 (cat. no. A09009; GenePharma) to evaluate its effect on TUBB4A promoter activity. After 48 h, both Firefly and *Renilla* luciferase activities were measured using the Dual-Luciferase Reporter Assay System (cat. no. E1910; Promega Corporation).

Chromatin immunoprecipitation (ChIP). ChIP analysis was performed to investigate endogenous STAT1 binding to the TUBB4A promoter. A375 and RPMI-7951 cells were cross-linked with 1% formaldehyde (cat. no. 28908; Thermo Fisher Scientific, Inc.) and lysed using SDS Lysis Buffer (cat. no. 20-163; Sigma-Aldrich; Merck KGaA) and chromatin was fragmented by sonication using a Bioruptor® PICO (cat. no. B01080010 Diagenode SA). For each reaction, 100 μg chromatin lysate was diluted to a final volume of 500 μl with ChIP dilution buffer and incubated with 5 μg of anti-STAT1 antibodies (1:100; cat. no. 14994; Cell Signaling Technology, Inc.) or control rabbit IgG (1:100; cat. no. 2729; Cell Signaling Technology, Inc.) overnight at 4˚C. Subsequently, ChIP-Grade Protein A/G Magnetic Beads (cat. no. 16-663; Sigma-Aldrich; Merck KGaA) were added according to the manufacturer's protocol. The immune complexes were washed sequentially with low and high salt buffer. The complexes were isolated by magnetic separation. DNA-protein complex crosslinking was reversed using proteinase K (cat. no. EO0491; Thermo Fisher Scientific, Inc.), and DNA was purified using the Aquadien DNA Purification kit (cat. no. 3578121; Bio-Rad Laboratories, Inc.). Quantitative PCR (qPCR) amplification of the TUBB4A promoter region was performed using SYBR® Green JumpStart™ Taq ReadyMix™ (cat. no. S4438; Sigma-Aldrich) on a CFX96 real-time PCR instrument (Bio-Rad). The thermocycling conditions were: 50˚C for 10 min, 95˚C for 5 min (1x), 95˚C for 10 sec/61˚C for 15 sec/72˚C for 30 sec (40x). The specific primer sequences for the *TUBB4A* promoter were: Forward 5'-CAGTGACCTGCA ACTGGAGA-3', reverse 5'-GATTGGCCAAACACGAAG TT-3'. Data were quantified using the %input method, where Input DNA (non-immunoprecipitated chromatin) served as the normalization control.

Mouse xenograft model. A total of 25 BALB/c nude mice (male; age, 8 weeks old, 23-25 g) were subcutaneously injected in the axillary region with $2x10^6$ A375 cells treated with si-STAT1 and Ov-TUBB4A, either separately or in combination, with 5 mice in each treatment group. BALB/c nude mice were purchased from Shanghai Bikai Keyi Biotechnology Co., Ltd (Shanghai, China). Mice were housed at a temperature of 22±2˚C, humidity of 55±5%, with a 12 h light/dark cycle. Food and water were provided *ad libitum*. Tumor volumes were measured every 3 days using calipers, and at the conclusion of the study, tumors were excised, weighed and photographed. At the experimental endpoint (five weeks after A375 cell injection), mice were sacrificed by overdose with sodium pentobarbital (150 mg/kg), with cervical dislocation . Humane endpoints for mice were as follows: i) Tumor size >1,500 mm^3; ii) ulceration, necrosis or infection were observed, particularly where the tumor broke the skin or became necrotic; iii) mice exhibited impaired mobility or interfered with normal functions, as indicated by the tumor location interfering with walking, feeding or drinking; iv) mice demonstrated signs of pain or distress, including hunched posture, lethargy, ruffled fur or abnormal vocalization; v) mice exhibited significant body weight loss, with a limit of >20% from a healthy control group adhered to; and vi) tumor growth interfered with vital organs and their functioning. No mice reached these experimental endpoints. Death was confirmed by the absence of a heartbeat and respiration for >5 min. All animal experiments were approved by the Institutional Animal Care and Use Committee of Pudong New Area People's Hospital (approval no. AEA-2024-33) and were conducted in accordance with ethical guidelines.

Statistical analysis. Data were presented as mean ± standard deviation from at least three independent experiments. Comparisons between groups were performed using paired

Student's t-test or one-way ANOVA followed by Tukey's honestly significant difference post hoc test. Correlations were analyzed using Pearson's coefficient. Survival analysis was conducted using Kaplan-Meier curves and the log-rank test, with statistical significance set at P<0.05.

Results

Expression and prognostic significance of TUBB4A in SKCM. Following queries concerning RNA sequencing data for TUBB4A and STAT1 expression in cancers, the GEPIA2 database revealed notably elevated TUBB4A expression in multiple tumor tissues compared with normal tissues, with data quantified in TPM. Specifically, in SKCM, TUBB4A expression was notably higher in tumor samples (TPM, 63.25) than in normal tissues (TPM, 1.52) (Fig. 1A). Box plot analysis further supported that tumor samples (n=461) exhibited significantly higher TUBB4A expression than normal samples (n=558) (P<0.05; Fig. 1B), suggesting that TUBB4A played a notable role in SKCM pathogenesis. Examination of TUBB4A expression across pathological stages 0-IV of SKCM (28) using a violin plot revealed no statistically significant differences between stages (F=2.25; P=0.0628; Fig. 1C). Kaplan-Meier survival analysis demonstrated that elevated TUBB4A expression (n=229) was strongly associated with reduced overall survival (OS) compared with low expression (n=229), with a log-rank P-value of $3.9x10^{-5}$ and a hazard ratio (HR) of 1.7 [p(hazard ratio, HR)=$4.9x10^{-5}$; Fig. 1D]. Additionally, high TUBB4A expression associated with significantly poorer disease-free survival (DFS), with a log-rank P-value of 0.013 and an HR of 1.4 (p(HR)=0.014; Fig. 1E). These results underscored the negative prognostic value of increased TUBB4A expression for both OS and DFS in patients with SKCM.

Correlation between STAT1 and TUBB4A expression in SKCM. The expression levels of STAT1 and TUBB4A in SKCM tissues were analyzed. Box plot analysis revealed significantly elevated STAT1 expression in cancerous tissues (n=461) compared with normal tissues (n=558) (P<0.05; Fig. 2A). STAT1 mRNA was also significantly upregulated in SKCM tumor tissues (n=31) compared with control tissues (n=31; P<0.05; Fig. 2B). Similarly, TUBB4A expression was significantly higher in SKCM tumor samples than in control tissue (P<0.05; Fig. 2C), indicating that both STAT1 and TUBB4A were upregulated in melanoma. Pearson's correlation analysis revealed a weak positive correlation between the mRNA expression of STAT1 and TUBB4A in SKCM (|R=0.4254|, R^2=0.1810; P=0.017; Fig. 2D), suggesting that STAT1 may have regulated TUBB4A expression. Further examination of STAT1 and TUBB4A levels in SKCM cell lines demonstrated significantly elevated STAT1 mRNA levels in the melanoma cell lines A2058, A375, RPMI-7951 and SK-MEL-1 compared with normal HEM (P<0.01; Fig. 2E), with A375 cells showing the highest STAT1 expression. Similarly, TUBB4A expression was significantly elevated in all melanoma cell lines relative to HEM (P<0.01), with the highest expression once again observed in A375 cells (Fig. 2F).

Silencing STAT1 markedly decreases the viability and proliferation of melanoma cells. To assess the impact of STAT1 knockdown on melanoma cells, STAT1 mRNA levels were measured in A375 and RPMI-7951 cell lines following transfection with si-STAT1. In both cell lines, STAT1 mRNA expression was significantly reduced in the si-STAT1 group compared with the control and si-NC groups (P<0.01), supporting the successful knockdown of STAT1 (Fig. 3A and B). At the protein level, western blot analysis further validated the knockdown of STAT1, revealing a notable decrease in STAT1 protein expression in both A375 and RPMI-7951 cells transfected with si-STAT1, while no significant changes were observed between the control and si-NC groups, reinforcing the effectiveness of the knockdown protocol (Fig. 3C). To investigate the functional consequences of STAT1 silencing, cell viability was assessed via CCK-8 assay. A significant reduction in cell viability over time was observed in the si-STAT1 group relative to the control and si-NC groups (P<0.01; Fig. 3D and E), suggesting that STAT1 was important for maintaining melanoma cell viability. Additionally, the si-STAT1 group exhibited a notable reduction in colony formation compared with the control and si-NC groups, indicating that STAT1 knockdown inhibited the proliferative capacity of melanoma cells. Quantitative analysis of colony formation assays further revealed a significant reduction in colony counts in both A375 and RPMI-7951 cell lines following transfection with si-STAT1 (P<0.01; Fig. 3F and G), reinforcing the conclusion that STAT1 downregulation suppressed melanoma cell proliferation.

Knockdown of STAT1 significantly promotes apoptosis and inhibits cell migration in melanoma cells. Apoptosis was assessed in A375 and RPMI-7951 cells following STAT1 knockdown using flow cytometry. Scatter plots revealed a significant increase in the proportion of cells undergoing apoptosis in the si-STAT1 group compared with the control groups, as indicated by a higher percentage of cells in the apoptotic region (Fig. 4A). Quantification of apoptotic rates showed that STAT1 knockdown significantly elevated apoptosis in both A375 and RPMI-7951 cells compared with the control and si-NC groups (P<0.05; Fig. 4B), suggesting that STAT1 knockdown promoted melanoma cell apoptosis. Furthermore, migration assays revealed a notable reduction in the number of migrating cells in the si-STAT1 group compared with the control and si-NC groups (Fig. 4C). Quantification of migrating cell counts supported that STAT1 knockdown significantly inhibited cell migration (P<0.05; Fig. 4D). Collectively, these results demonstrated that STAT1 was important for the viability, proliferation and migration of melanoma cells, with its depletion promoting apoptosis and inhibiting cell migration. These results underscored the notable role of STAT1 in regulating melanoma cell survival and migratory capacity.

STAT1 regulates the expression of TUBB4A through transcriptional mechanisms. Two independent si-STAT1 sequences, denoted si-STAT1-1 and si-STAT1-2, were utilized for transfection. qPCR analyses demonstrated that both siRNA sequences induced a significant reduction in STAT1 mRNA level (P<0.01; Fig. 5A), whereas the si-NC sequence exerted no significant effects on STAT1 expression. Following STAT1 knockdown, a significant reduction in

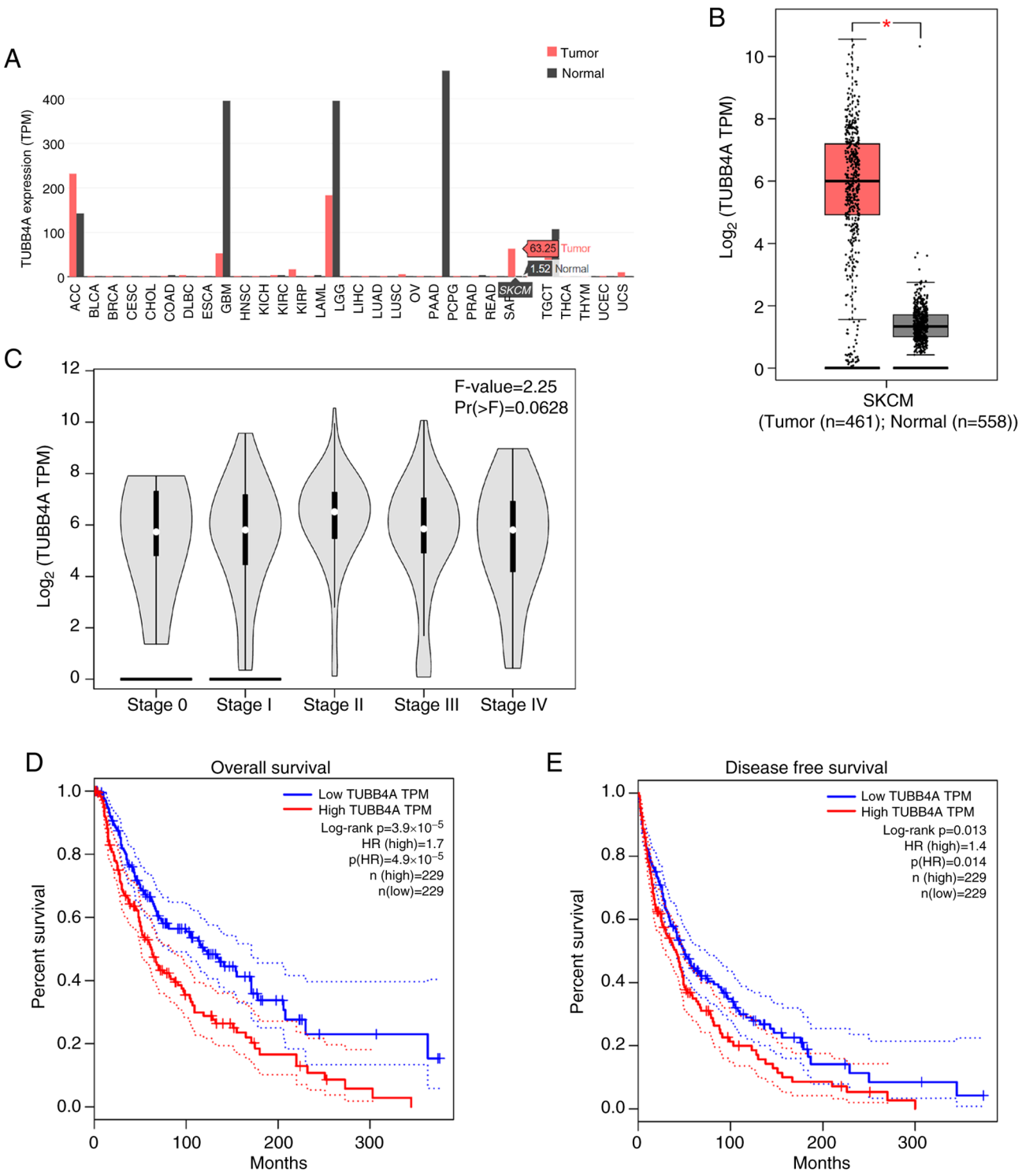

Figure 1. Bioinformatic analysis demonstrates elevated TUBB4A expression in melanoma, correlating with poor prognosis. (A) Data from the Gene Expression Profiling Interactive Analysis 2 database revealed that TUBB4A was markedly altered across various cancers, with a marked upregulation in SKCM. (B) Further comparison of TUBB4A expression in melanoma tissues vs. control tissues highlighted a significant increase in TUBB4A levels in melanoma samples. (C) Analysis of TUBB4A expression across different melanoma stages revealed no significant variation in expression levels. Kaplan-Meier survival analysis measuring TUBB4A expression against (D) overall survival and (E) disease-free survival showed that high TUBB4A expression was significantly associated with poorer overall survival and disease-free survival outcomes, compared with patients demonstrating low TUBB4A expression. *P<0.05. SKCM, skin cutaneous melanoma; TUBB4A, tubulin β4A; TPM, transcripts per million; HR, hazard ratio.

TUBB4A mRNA expression was observed in both A375 and RPMI-7951 melanoma cells compared with the si-NC group (P<0.01; Fig. 5B). Bioinformatic analysis identified multiple high-confidence STAT1 binding motifs within the regulatory region of the TUBB4A promoter (Table SII). These motifs were selected for further experimental validation. A series of luciferase reporter constructs containing TUBB4A promoter fragments were generated, spanning from -2,000 to -32 base pairs relative to the transcription initiation site (Fig. 5C). Reporter assays revealed that the -1,783 and -1,771 fragments

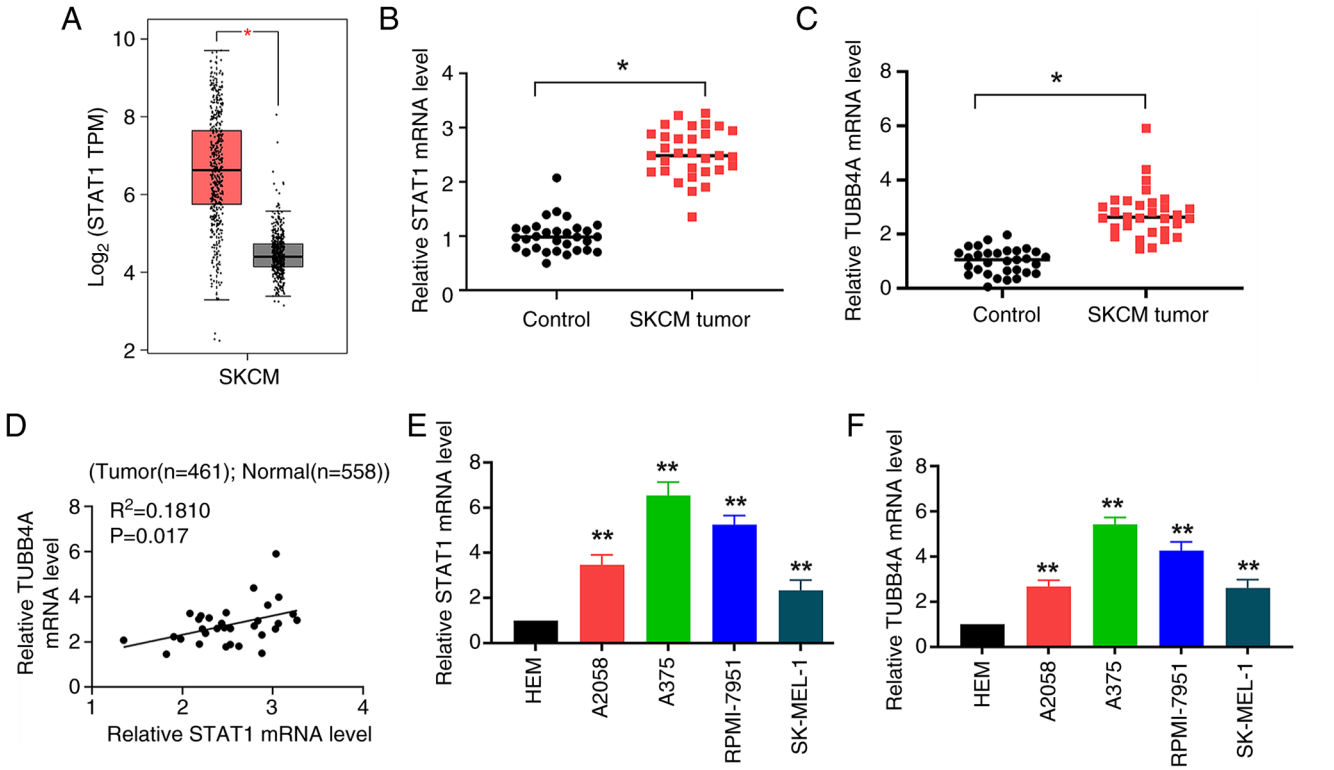

Figure 2. STAT1 and TUBB4A expression levels are significantly correlated and upregulated in melanoma. (A) Analysis of data in the Gene Expression Profiling Interactive Analysis 2 database revealed a significant elevation of STAT1 expression in melanoma tissues. Quantification of (B) STAT1 and (C) TUBB4A mRNA levels in 31 paired melanoma and normal tissue samples from patients with SKCM demonstrated a significant upregulation of both STAT1 and TUBB4A expression in melanoma tissues. (D) Correlation analysis of STAT1 and TUBB4A mRNA levels in melanoma samples showed a significant positive correlation. Comparative analysis of (E) STAT1 and (F) TUBB4A mRNA expression in normal HEM and melanoma cell lines revealed significantly higher expression in the melanoma cell lines. *P<0.05 between groups; **P<0.01 compared with HEM cells. HEM, human epidermal melanocytes; STAT1, signal transducer and activator of transcription 1; TUBB4A, tubulin β4A; TPM, transcripts per million; SKCM, skin cutaneous melanoma.

exhibited the highest transcriptional activity, as indicated by significantly increased luciferase activity relative to other fragments (P<0.01; Fig. 5D). These results suggested that the -1,783 and -1,771 regions were important for TUBB4A promoter activity. The mRNA results validated the efficacy of STAT1 knockdown (Fig. 5E). Upon STAT1 knockdown, luciferase activity of the promoter-gluc luciferase (PGL)3-1783 construct significantly decreased (P<0.01; Fig. 5F), while the PGL3-1771 construct showed no significant changes in luciferase activity. This suggested that STAT1 specifically regulated transcription through the -1,783 region of the TUBB4A promoter. ChIP assays further supported that STAT1 binding to the TUBB4A promoter was significantly enriched at the -1,783 region in both A375 and RPMI-7951 cells compared with IgG control (P<0.01; Fig. 5G), providing direct evidence that STAT1 interacted with the TUBB4A promoter at this site. These results demonstrated that STAT1 directly regulated TUBB4A expression at the transcriptional level by binding to the -1,783 region of the TUBB4A promoter.

TUBB4A overexpression partially reverses the suppressive impact of STAT1 knockdown on cell viability. Compared with the control and Ov-NC groups, the Ov-TUBB4A group exhibited a significant increase in TUBB4A expression (P<0.01; Fig. 6A and B), providing evidence of successful overexpression. Western blot analysis further validated TUBB4A overexpression in A375 and RPMI-7951 cells, with a marked increase in TUBB4A protein levels observed in the Ov-TUBB4A group relative to the control and Ov-NC groups (Fig. 6C), supporting effective protein overexpression. TUBB4A protein levels were also assessed under various conditions, including combined STAT1 knockdown and TUBB4A overexpression (Fig. 6D and E). To assess the impact of STAT1 knockdown and TUBB4A overexpression on cell proliferation, CCK-8 assays were conducted in A375 and RPMI-7951 cells. As aforementioned, STAT1 knockdown significantly decreased cell viability in both cell lines. Conversely, TUBB4A overexpression significantly rescued cell proliferation (P<0.01; Fig. 6F and G). STAT1 knockdown led to a notable reduction in colony formation, indicating impaired proliferative capacity in STAT1-deficient melanoma cells. However, simultaneous overexpression of TUBB4A markedly restored colony formation compared with the si-STAT1 group (Fig. 6H). Quantitative colony formation analysis supported a significant reduction in colony formation in the si-STAT1 group, with TUBB4A overexpression significantly restoring colony formation (P<0.01; Fig. 6I). These results demonstrated that STAT1 silencing significantly inhibited melanoma cell proliferation and colony formation in both A375 and RPMI-7951 cells, while TUBB4A overexpression partially reversed these effects, suggesting that TUBB4A functioned as a downstream effector of STAT1, playing a compensatory role in regulating melanoma cell proliferation and survival.

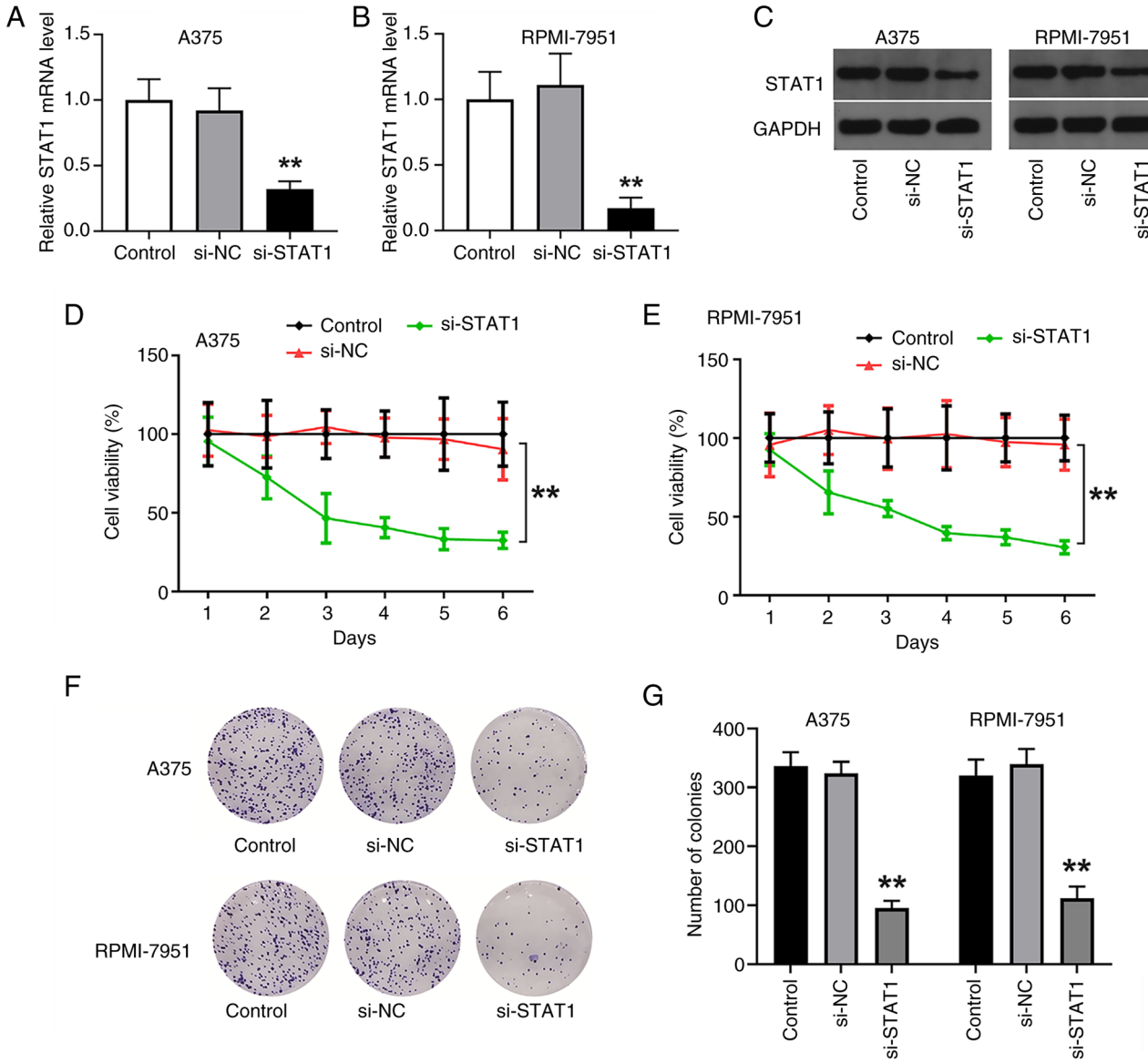

Figure 3. STAT1 knockdown significantly reduces melanoma cell viability and proliferation. STAT1 mRNA expression was analyzed in (A) A375 and (B) RPMI-7951 melanoma cells post-STAT1 knockdown using siRNA. (C) Western blotting was used to assess STAT1 protein levels in melanoma cell lines following siRNA-mediated knockdown. Cell viability was evaluated after STAT1 knockdown in (D) A375 and (E) RPMI-7951 cells using Cell Counting Kit-8 assays. (F) Colony formation assays were performed to assess the proliferative capacity of cells after STAT1 knockdown. (G) Quantification of colony formation assay results. **P<0.01 vs. si-NC group. siRNA, small interfering RNA; STAT1, signal transducer and activator of transcription 1; si-STAT1, siRNA targeting STAT1; si-NC, negative control siRNA.

Overexpression of TUBB4A partially reverses the effect of STAT1 knockdown on cell apoptosis, migration and tumor growth in vivo. Flow cytometric analysis was conducted to evaluate apoptosis in A375 cells following transfection treatments. STAT1 knockdown markedly increased the apoptotic rate compared with the control and si-NC groups. However, co-transfection with TUBB4A overexpression vectors partially mitigated this apoptotic effect, as evidenced by a notable reduction in apoptotic cells (Fig. 7A). Quantification of apoptotic rates supported a significant increase in apoptosis in the si-STAT1 group compared with the si-NC group, while the si-STAT1 + Ov-TUBB4A group showed a significant reduction in apoptosis compared with STAT1 knockdown alone (P<0.01; Fig. 7C). These results suggested that TUBB4A overexpression counterbalanced the elevation in apoptosis induced by STAT1 knockdown. To assess the effects of STAT1 knockdown and TUBB4A overexpression on cell migration, Transwell assays were performed in RPMI-7951 cells (Fig. 7B). STAT1 knockdown markedly inhibited cell migration, as demonstrated by the reduced number of migrating cells. Notably, TUBB4A overexpression following STAT1 knockdown partially restored migration, indicating a potential rescue effect. Quantitative migration analysis revealed a significant reduction in the number of migrating cells in the si-STAT1 group compared with the si-NC group, while this migration ability was partially yet significantly restored in the si-STAT1 + Ov-TUBB4A group (P<0.01; Fig. 7D), suggesting that TUBB4A overexpression partially counteracted the inhibitory effect of STAT1 knockdown on melanoma cell migration.

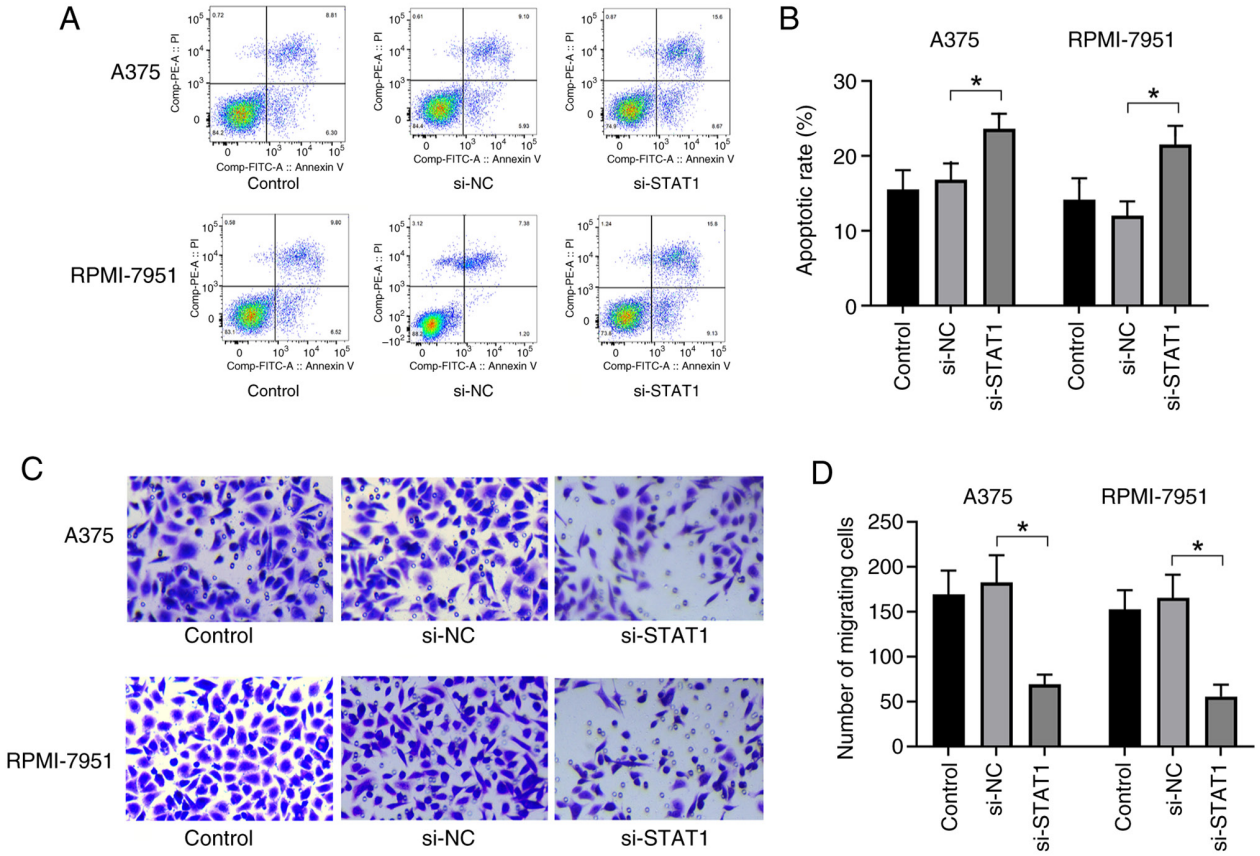

Figure 4. STAT1 knockdown significantly promotes melanoma cell apoptosis and inhibits migration. (A and B) Apoptosis was assessed and quantified in A375 and RPMI-7951 cells following STAT1 knockdown using flow cytometry. (C) Transwell migration assays were conducted to evaluate cell migration following STAT1 knockdown. Magnification, x200. (D) Quantification of migration capacity in A375 and RPMI-7951 cells following STAT1 knockdown. *P<0.05 vs. si-NC. STAT1, signal transducer and activator of transcription 1; si-STAT1, small interfering RNA targeting STAT1; si-NC, negative control small interfering RNA.

In vivo tumorigenicity assays were performed by injecting A375 cells into mice. Tumors derived from the si-STAT1 group were notably smaller than those from the control and si-NC groups, indicating that STAT1 knockdown markedly suppressed tumor growth. However, tumor volume in the si-STAT1 + Ov-TUBB4A group was notably larger compared with the si-STAT1 group (Fig. 7E), suggesting that TUBB4A overexpression partially rescued the tumor growth inhibition caused by STAT1 knockdown. Quantitative analysis supported a significant reduction in tumor volume in the si-STAT1 group compared with the si-NC group, while the si-STAT1 + Ov-TUBB4A group exhibited a significantly larger tumor volume than the si-STAT1 group (P<0.01; Fig. 7F). The maximum tumor volume and diameter observed at the endpoint of the study were 1,320 mm^3 and 13.6 mm, respectively, which were observed in the si-NC group. These results further supported the conclusion that TUBB4A overexpression mitigated the suppressive effects of STAT1 knockdown on tumor growth. Collectively, these results suggested that TUBB4A may have functionally cooperated with STAT1 to regulate apoptosis, migration and tumor growth in melanoma cells.

Discussion

Melanoma, an aggressive form of skin cancer, presents ongoing challenges in clinical management. The present study explored the complex roles of STAT1 and TUBB4A in SKCM, focusing on their involvement in regulating cell proliferation, migration, apoptosis and tumor progression. The findings of the present study underscored the important role of STAT1 in promoting melanoma progression through its regulation of cell survival and motility, while TUBB4A served as a downstream effector that mitigated the adverse effects of STAT1 silencing in melanoma cells.

The present results aligned with previous studies highlighting STAT1 as an important regulator of tumor progression. STAT1 regulates numerous cellular processes, including immune responses, proliferation and apoptosis (29-31). In melanoma, STAT1 upregulation is associated with favorable or poor prognosis, reflecting its dual role as either a tumor suppressor or promoter, depending on the tumor context (15,32). In the present study, silencing STAT1 significantly impaired melanoma cell proliferation, migration and colony formation, while simultaneously promoting apoptosis. These findings demonstrated that STAT1 supported melanoma cell survival and motility, consistent with observations in other cancer types where STAT1 facilitates tumor invasion and metastasis (33,34). An apoptotic rate of ~20% following STAT1 knockdown, while modest in absolute terms, reflected a strong 3-4 fold increase over control levels. Similar ranges of apoptotic induction following specific gene knockdown, with rates ranging from 15-30%, have been

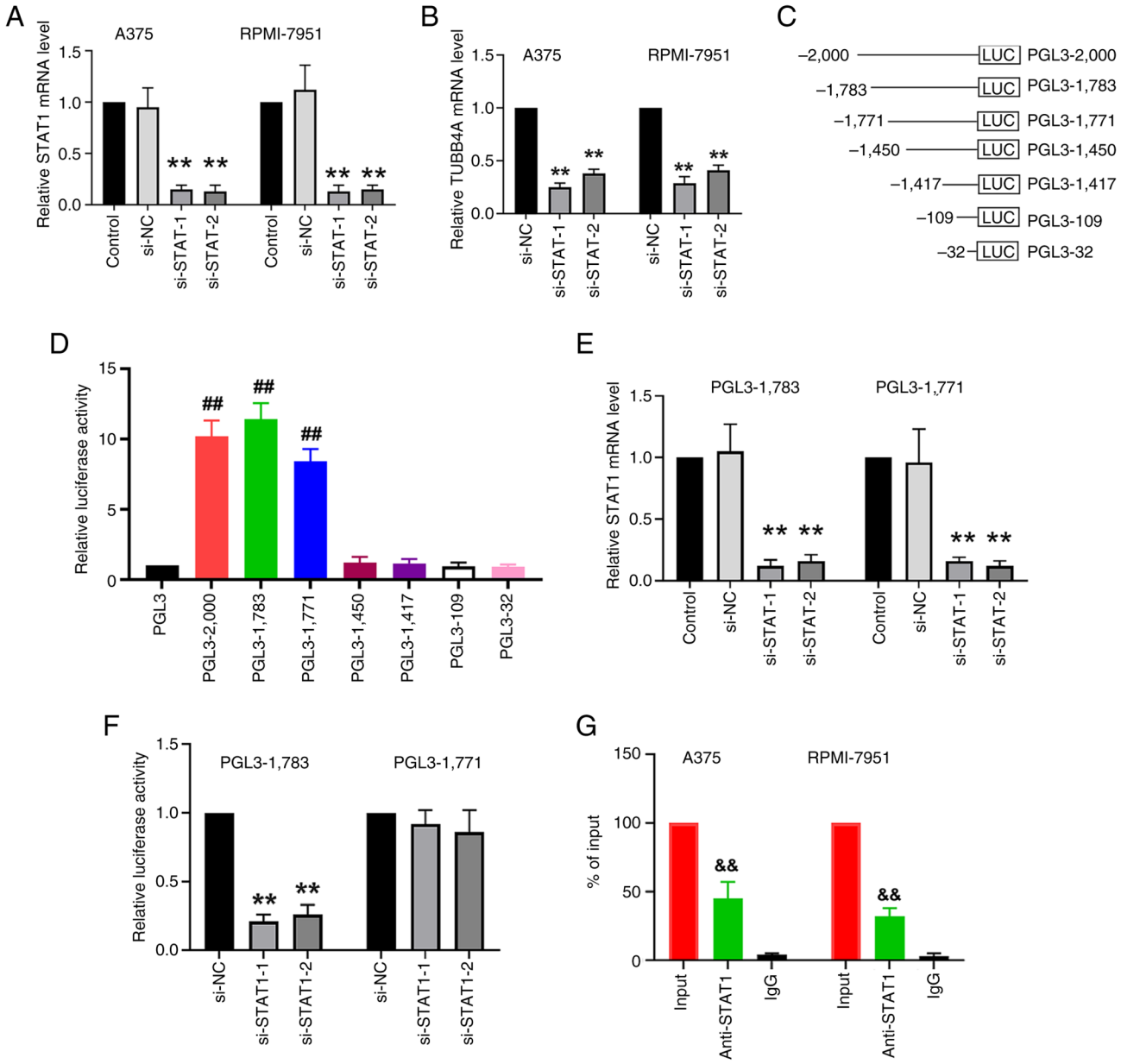

Figure 5. STAT1 regulates TUBB4A expression at the transcription level. (A) STAT1 mRNA levels were measured in A375 and RPMI-7951 cells after STAT1 knockdown via transfection with different siRNA sequences. (B) TUBB4A mRNA levels were measured in A375 and RPMI-7951 cells after STAT1 knockdown via transfection with different siRNA sequences. (C) Specific fragments of the TUBB4A promoter region were cloned into the luciferase reporter plasmids upstream of the firefly luciferase gene. (D) Transcriptional activity of various TUBB4A promoter fragments was analyzed by luciferase reporter assay in 293T cells, with the -1,783 and -1,771 fragments exhibiting the highest activity. (E) STAT1 siRNA-mediated knockdown significantly reduced STAT1 mRNA levels in A375 cells. (F) STAT1 knockdown significantly reduced the luciferase activity of the -1,783 fragment of the TUBB4A promoter, but not the -1,771 fragment. (G) Chromatin immunoprecipitation assays were performed in A375 and RPMI-7951 cells targeting the -1,783 binding site in the TUBB4A promoter region. Quantitative PCR provided evidence of STAT1 binding to this region. Genomic DNA input was set to 100%. **P<0.01 vs. si-NC; $^{\#\#}$P<0.01 vs. PGL3; $^{\&\&}$P<0.01 vs. IgG. STAT1, signal transducer and activator of transcription 1; siRNA, small interfering RNA; si-NC, negative control siRNA; si-STAT1, siRNA targeting STAT1; si-STAT1-1, siRNA targeting STAT1 sequence 1; si-STAT1-2, siRNA targeting STAT1 sequence 2; TUBB4A, tubulin β4A; PGL3, promoter-gluc luciferase 3; LUC, firefly luciferase gene.

frequently reported in cancer research literature and are accepted as evidence of the notable role of a gene in cell survival (35-38). In the context of single-gene manipulation without additional cytotoxic agents, the discussed magnitude of change is biologically notable and consistent with the profound reductions observed in cell viability and long-term proliferation in the present study, robustly supporting the conclusion that STAT1 was important for melanoma cell survival.

Notably, the role of STAT1 in melanoma contrasted with its generally tumor-suppressive function in cancers such as breast and colorectal cancer (39-42). This divergence suggested that the effects of STAT1 may have been context-dependent, with its contribution to melanoma progression likely modulated by interactions with other oncogenic pathways. Although STAT1 is recognized for its role in orchestrating anti-tumor immune responses and inflammation (43), the findings of the present study, consistent with

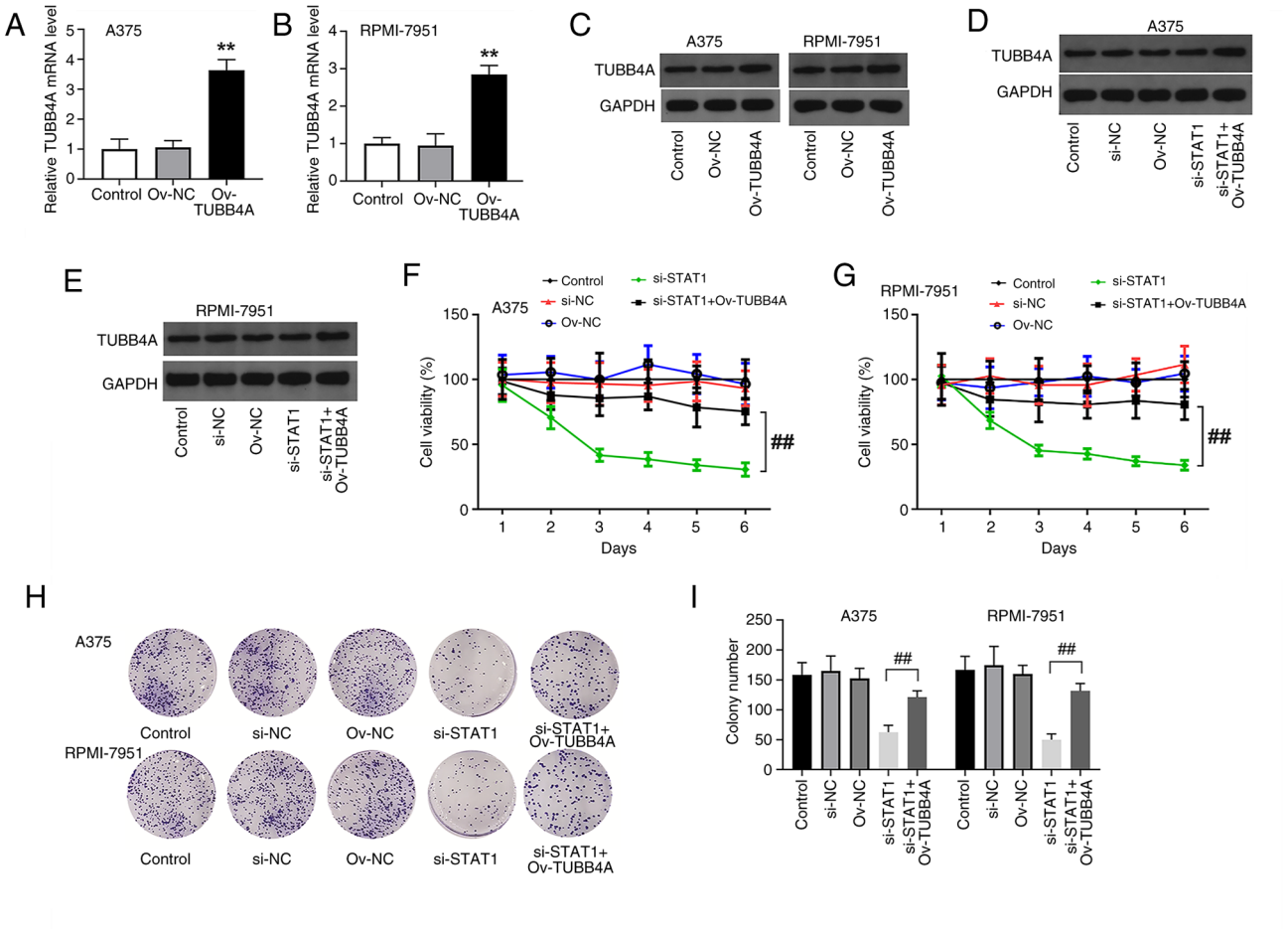

Figure 6. TUBB4A overexpression mitigates the effects of STAT1 knockdown on cell viability and proliferation. TUBB4A mRNA levels were measured in (A) A375 and (B) RPMI-7951 cells following TUBB4A overexpression mediated by a lentiviral vector. (C) TUBB4A protein expression was analyzed after its overexpression. Combined STAT1 knockdown and TUBB4A overexpression transfections were performed, followed by a western blot analysis of TUBB4A protein levels in (D) A375 and (E) RPMI-7951 cells. Cell viability was assessed via Cell Counting Kit-8 assays following combined STAT1 knockdown and TUBB4A overexpression in (F) A375 and (G) RPMI-7951 cells. (H) Colony formation assays were performed to assess the proliferative capacity of cells after STAT1 knockdown and TUBB4A overexpression. (I) Quantification of colony formation assay results. **P<0.01 vs. Ov-NC; $^{\#\#}$P<0.01 vs. si-STAT1. TUBB4A, tubulin β4A; STAT1, signal transducer and activator of transcription 1; si-NC, negative control small interfering RNA; si-STAT1, small interfering RNA targeting STAT1; Ov-NC, negative control lentiviral overexpression vector; Ov-TUBB4A, lentiviral vector for TUBB4A overexpression.

emerging evidence in melanoma (6,15,32), underscored its context-dependent oncogenic capacity. The pro-tumorigenic role of STAT1 may have extended beyond the regulation of cell proliferation and apoptosis. Notable evidence indicates that STAT1 serves as a core transcription factor in the IFNγ signaling pathway and directly participates in regulating the expression of the immune checkpoint molecule programmed cell death 1 ligand 1 (PD-L1) (44-46). A previous study in aggressive soft-tissue sarcomas also revealed co-expression of PD-L1 with cancer-testis antigens such as cancer-testis antigen 1, suggesting a potential role for the STAT1 pathway in shaping the tumor immune microenvironment (47). Therefore, the present study speculated that in melanoma, STAT1 activation may have concurrently driven malignant progression and immune escape. Targeting STAT1 could potentially kill tumor cells directly by inhibiting the expression of downstream targets such as TUBB4A; on the other hand, targeting STAT1 may enhance T-cell-mediated cytotoxicity by downregulating molecules such as PD-L1. Therefore, the results of the present study provided a theoretical foundation for combining STAT1 inhibitors with immune checkpoint blockers. This combinatorial strategy represents an important direction for future research.

The present study elucidated a novel mechanism through which STAT1 drove melanoma progression by upregulating TUBB4A expression. The significant association between high STAT1 expression and poor patient survival, coupled with mechanistic data identifying the pro-survival and pro-migratory factor TUBB4A as a direct transcriptional target of STAT1, suggested that in melanoma, the tumor-promoting functions of STAT1 overrode its classical tumor-suppressive roles. Kaplan-Meier survival analysis demonstrated that elevated TUBB4A expression was strongly associated with reduced OS and DFS, underscoring its negative prognostic value. Notably, while TUBB4A expression was significantly elevated in melanoma tissues overall, the cross-stage analysis performed in the present study did not detect statistically significant variations in its expression levels. This suggested that TUBB4A upregulation was an early event in melanomagenesis, remaining relatively stable throughout disease progression. However, the present study could not rule out the possibility that subtle changes in TUBB4A expression existed

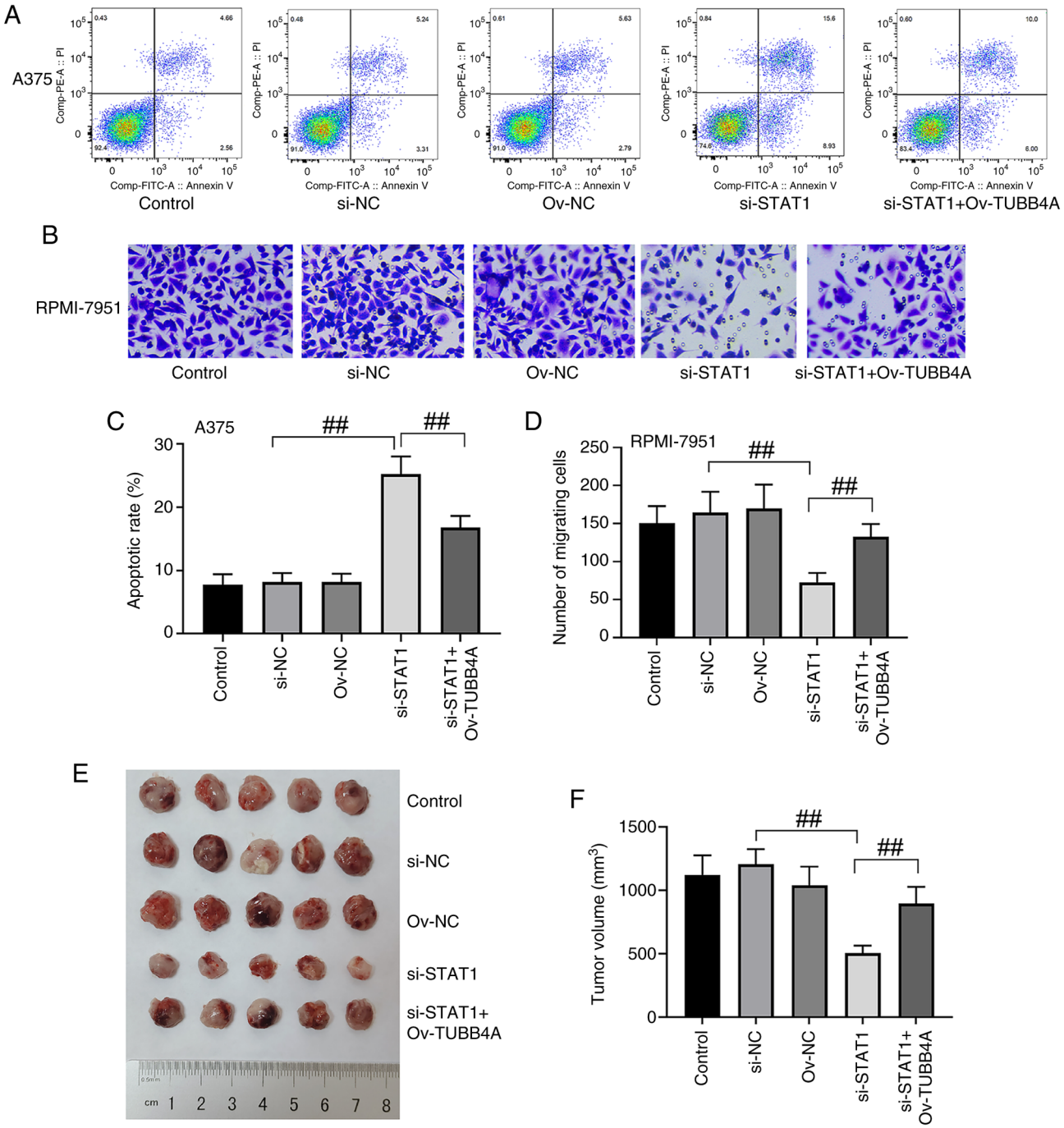

Figure 7. TUBB4A overexpression reverses the effects of STAT1 knockdown on apoptosis, migration and tumor growth. (A-D) Apoptosis and migration were evaluated in A375 and RPMI-7951 cells following STAT1 knockdown and TUBB4A overexpression. Magnification, x200. (E) Representative images of isolated xenograft tumors in mice. Tumor volumes were measured in nude mice injected subcutaneously with $2x10^6$ A375 cells that had been subject to STAT1 knockdown and TUBB4A overexpression. (F) Quantification of mouse tumor volumes showed that STAT1 knockdown significantly suppressed tumor growth, whereas TUBB4A overexpression reversed this inhibitory effect. $^{\#\#}P<0.01$ vs. si-STAT1. TUBB4A, tubulin β4A; si-NC, negative control small interfering RNA; Ov-TUBB4A, lentiviral vector for TUBB4A overexpression.

but were not captured due to the sample size distribution across stages. The consistent high expression of TUBB4A, irrespective of pathological stage, further supported its potential role as a fundamental driver of melanoma progression.

The analysis of STAT1-TUBB4A interactions conducted within the present study revealed that the overexpression of TUBB4A partially reversed the inhibitory effects of STAT1 knockdown on cell proliferation, migration and colony formation. These findings suggested that TUBB4A acted as a compensatory factor in melanoma cells under conditions of STAT1 silencing. As a notable component of the microtubule network, TUBB4A is important for maintaining cell integrity and supports cellular processes such as division, migration and survival (8,48). The present results suggested that TUBB4A played a notable role in melanoma cell migration and apoptosis, likely by stabilizing microtubules and influencing cytoskeletal dynamics. The interplay between STAT1 and TUBB4A in melanoma pointed to a potential mechanism in which

STAT1 drove tumor progression by upregulating TUBB4A. In turn, TUBB4A appeared to support tumor cell migration and survival by stabilizing microtubules, remodeling the cytoskeleton and enhancing motility (49). This was consistent with findings in other types of cancer, where tubulin family proteins, including TUBB4A, and microtubule dynamics contribute to tumor growth and therapy resistance (50).

In vivo experiments further demonstrated that TUBB4A overexpression partially reversed the reduction in tumor size induced by STAT1 knockdown. While tumor growth was not fully restored to baseline, these results suggested that TUBB4A supported tumor maintenance by promoting cell proliferation and survival within the tumor microenvironment. The incomplete reversal of tumor growth highlighted that additional molecular mechanisms were potentially involved in melanoma progression and that TUBB4A alone could not fully compensate for STAT1 silencing. This underscores the complexity of tumor biology, where multiple pathways and factors collaboratively influence cancer development (51). Future research should explore the interactions of TUBB4A with other key molecules, such as STAT3 and additional tubulin family proteins, to further elucidate its role in melanoma progression.

The present study elucidated a novel mechanism whereby STAT1 drove melanoma progression through the direct transcriptional upregulation of TUBB4A. Placing this newly identified axis in context alongside the well-established oncogene STAT3 in melanoma helps to further define the findings of the present study. STAT3 plays a central role in promoting cell survival, proliferation and immune evasion by upregulating target genes such as *Bcl-xL,* Myeloid cell leukemia-1, *c-Myc* and *cyclin D1* (52-54). Although STAT1 and STAT3 are structurally related and can be activated by overlapping upstream signals, for example through shared cytokine receptors such as gp130, they often exhibit antagonistic or divergent functions in melanoma (55,56). The present finding that STAT1 exerted its pro-tumorigenic effect by regulating TUBB4A, a key gene involved in microtubule dynamics and cell motility, suggested a distinct mechanism through which STAT1 drove malignancy, potentially independent of the canonical STAT3 signaling network. Nonetheless, potential synergy cannot be ruled out; STAT1 and STAT3 may cooperate to promote aggressiveness and therapy resistance in melanoma by regulating separate yet complementary sets of downstream targets. A key source of ambiguity in the present study was whether TUBB4A was a shared target or was specifically regulated by STAT1, which will be a focus of our future investigations. In summary, the present study uncovered a previously underappreciated, non-canonical oncogenic role for STAT1 in melanoma, independent of its classic immune-related functions, and added a new layer of complexity to the STAT signaling paradigm by identifying TUBB4A as a key downstream effector.

Given the role of TUBB4A in melanoma, further studies are necessary to elucidate its underlying molecular mechanisms, particularly in relation to tumor-associated signaling pathways. Investigating the interaction between TUBB4A and STAT3, a notable regulator in melanoma progression, could offer valuable insights into how these molecules collaborate in tumor development. Additionally, exploring how TUBB4A influences the tumor microenvironment, including immune responses and metastatic potential, may reveal novel therapeutic targets. The present study also emphasized the therapeutic potential of targeting the STAT1-TUBB4A axis. Since TUBB4A is implicated in drug resistance across various cancers, its contribution to the resistance of melanoma to chemotherapy and immunotherapy warrants in-depth exploration. A combined approach targeting both STAT1 and TUBB4A may present an innovative strategy to overcome therapeutic resistance and enhance treatment outcomes for patients with melanoma.

Summarily, STAT1 drove melanoma progression by upregulating TUBB4A expression, with TUBB4A acting as a downstream effector. The capacity of TUBB4A to counteract the effects of STAT1 knockdown underscored the potential of the STAT1-TUBB4A axis as a therapeutic target in melanoma. These findings provided valuable insights into refining treatment strategies for melanoma, highlighting the importance of targeting this pathway to enhance therapeutic efficacy.

Acknowledgements

Not applicable.

Funding

No funding was received.

Availability of data and materials

The data generated in the present study may be requested from the corresponding author.

Authors' contributions

RZ and KF designed the study, performed *in vitro* experiments and analyzed data. XZ contributed to patient sample collection and clinical data interpretation. HL supervised the project, designed *in vivo* xenograft experiments and interpreted results. RZ and HL drafted the manuscript. KF and XZ prepared figures and revised the manuscript. RZ and HL confirm the authenticity of all the raw data. All authors read and approved the final version of the manuscript.

Ethics approval and consent to participate

Approval for clinical and animal experimental protocols was granted by the Ethics Committee of Pudong New Area People's Hospital (animal study, approval no. AEA-2024-33; clinical sample study, approval no. CEA-2023-16). The requirement for ethical approval regarding the use of primary human epidermal melanocytes in the present study was waived by the Ethics Committee of Pudong New Area People's Hospital. All subjects involved in the study provided informed consent. Patients provided written consent for participation in the present study.

Patient consent for publication

Not applicable.

Competing interests

The authors declare that they have no competing interests.

References

1. Liu M, Wu M, Liu X, Zhou J, Lan Y, Zhang H, Zhang X, Leng L, Zheng H and Li J: Assessing the quality of care for skin malignant melanoma on a global, regional, and national scale: A systematic analysis of the global burden of disease study from 1990 to 2019. Arch Dermatol Res 315: 2893-2904, 2023.
2. Arnold M, Singh D, Laversanne M, Vignat J, Vaccarella S, Meheus F, Cust AE, de Vries E, Whiteman DC and Bray F: Global burden of cutaneous melanoma in 2020 and projections to 2040. JAMA Dermatol 158: 495-503, 2022.
3. Sarapultsev A, Gusev E, Komelkova M, Utepova I, Luo S and Hu D: JAK-STAT signaling in inflammation and stress-related diseases: Implications for therapeutic interventions. Mol Biomed 4: 40, 2023.
4. Xue C, Yao Q, Gu X, Shi Q, Yuan X, Chu Q, Bao Z, Lu J and Li L: Evolving cognition of the JAK-STAT signaling pathway: autoimmune disorders and cancer. Signal Transduct Target Ther 8: 204, 2023.
5. Wang W, Lopez McDonald MC, Kim C, Ma M, Pan ZT, Kaufmann C and Frank DA: The complementary roles of STAT3 and STAT1 in cancer biology: Insights into tumor pathogenesis and therapeutic strategies. Front Immunol 14: 1265818, 2023.
6. Huang L, Chen J, Zhao Y, Gu L, Shao X, Li J, Xu Y, Liu Z and Xu Q: Key candidate genes of STAT1 and CXCL10 in melanoma identified by integrated bioinformatical analysis. IUBMB Life 71: 1634-1644, 2019.
7. Isacescu E, Chiroi P, Zanoaga O, Nutu A, Budisan L, Pirlog R, Atanasov AG and Berindan-Neagoe I: Melanoma cellular signaling transduction pathways targeted by polyphenols action mechanisms. Antioxidants (Basel) 12: 407, 2023.
8. Gao S, Wang S, Zhao Z, Zhang C, Liu Z, Ye P, Xu Z, Yi B, Jiao K, Naik GA, *et al*: TUBB4A interacts with MYH9 to protect the nucleus during cell migration and promotes prostate cancer via GSK3β/β-catenin signalling. Nat Commun 13: 2792, 2022.
9. Kanakkanthara A and Miller JH: βIII tubulin overexpression in cancer: Causes, consequences, and potential therapies. Biochim Biophys Acta Rev Cancer 1876: 188607, 2021.
10. Novikov NM, Zolotaryova SY, Gautreau AM and Denisov EV: Mutational drivers of cancer cell migration and invasion. Br J Cancer 124: 102-114, 2021.
11. Thomas SJ, Snowden JA, Zeidler MP and Danson SJ: The role of JAK/STAT signalling in the pathogenesis, prognosis and treatment of solid tumours. Br J Cancer 113: 365-371, 2015.
12. Hu X, Li J, Fu M, Zhao X and Wang W: The JAK/STAT signaling pathway: From bench to clinic. Signal Transduct Target Ther 6: 402, 2021.
13. Hu Q, Bian Q, Rong D, Wang L, Song J, Huang HS, Zeng J, Mei J and Wang PY: JAK/STAT pathway: Extracellular signals, diseases, immunity, and therapeutic regimens. Front Bioeng Biotechnol 11: 1110765, 2023.
14. Gandalovicova A, Šůchová AM, Čermák V, Merta L, Rösel D and Brábek J: Sustained inflammatory signalling through Stat1/Stat2/IRF9 is associated with amoeboid phenotype of melanoma cells. Cancers (Basel) 12: 2450, 2020.
15. Osborn JL and Greer SF: Metastatic melanoma cells evade immune detection by silencing STAT1. Int J Mol Sci 16: 4343-4361, 2015.
16. Wang W, Lopez McDonald MC, Hariprasad R, Hamilton T and Frank DA: Oncogenic STAT transcription factors as targets for cancer therapy: Innovative strategies and clinical translation. Cancers (Basel) 16: 1387, 2024.
17. Prutsch N, He S, Berezovskaya A, Durbin AD, Dharia NV, Maher KA, Matthews JD, Hare L, Turner SD, Stegmaier K, *et al*: STAT3 couples activated tyrosine kinase signaling to the oncogenic core transcriptional regulatory circuitry of anaplastic large cell lymphoma. Cell Rep Med 5: 101472, 2024.
18. Fu XQ, Liu B, Wang YP, Li JK, Zhu PL, Li T, Tse KW, Chou JY, Yin CL, Bai JX, *et al*: Activation of STAT3 is a key event in TLR4 signaling-mediated melanoma progression. Cell Death Dis 11: 246, 2020.
19. Kortylewski M, Jove R and Yu H: Targeting STAT3 affects melanoma on multiple fronts. Cancer Metastasis Rev 24: 315-327, 2005.
20. Chen J, Kholina E, Szyk A, Fedorov VA, Kovalenko I, Gudimchuk N and Roll-Mecak A: α-tubulin tail modifications regulate microtubule stability through selective effector recruitment, not changes in intrinsic polymer dynamics. Dev Cell 56: 2016-2028.ed, 2021.
21. Fu G, Yan S, Khoo CJ, Chao VC, Liu Z, Mukhi M, Hervas R, Li XD and Ti SC: Integrated regulation of tubulin tyrosination and microtubule stability by human alpha-tubulin isotypes. Cell Rep 42: 112653, 2023.
22. Garcin C and Straube A: Microtubules in cell migration. Essays Biochem 63: 509-520, 2019.
23. Nami B and Wang Z: Genetics and expression profile of the tubulin gene superfamily in breast cancer subtypes and its relation to taxane resistance. Cancers (Basel) 10: 274, 2018.
24. Song JX, Wang Y, Hua ZP, Huang Y, Hu LF, Tian MR, Qiu L, Liu H and Zhang J: FATS inhibits the Wnt pathway and induces apoptosis through degradation of MYH9 and enhances sensitivity to paclitaxel in breast cancer. Cell Death Dis 15: 835, 2024.
25. Wagstaff W, Mwamba RN, Grullon K, Armstrong M, Zhao P, Hendren-Santiago B, Qin KH, Li AJ, Hu DA, Youssef A, *et al*: Melanoma: Molecular genetics, metastasis, targeted therapies, immunotherapies, and therapeutic resistance. Genes Dis 9: 1608-1623, 2022.
26. Marconcini R, Pezzicoli G, Stucci LS, Sergi MC, Lospalluti L, Porta C and Tucci M: Combination of immunotherapy and other targeted therapies in advanced cutaneous melanoma. Hum Vaccin Immunother 18: 1980315, 2022.
27. Livak KJ and Schmittgen TD: Analysis of relative gene expression data using real-time quantitative PCR and the 2(-Delta Delta C(T)) method. Methods 25: 402-408, 2001.
28. Papageorgiou C, Apalla Z, Manoli SM, Lallas K, Vakirlis E and Lallas A: Melanoma: Staging and follow-up. Dermatol Pract Concept 11(Suppl): e2021162S, 2021.
29. Tolomeo M, Cavalli A and Cascio A: STAT1 and its crucial role in the control of viral infections. Int J Mol Sci 23: 4095, 2022.
30. Niu M, Yi M, Dong B, Luo S and Wu K: Upregulation of STAT1-CCL5 axis is a biomarker of colon cancer and promotes the proliferation of colon cancer cells. Ann Transl Med 8: 951, 2020.
31. Li X, Wang F, Xu X, Zhang J and Xu G: The dual role of STAT1 in ovarian cancer: Insight into molecular mechanisms and application potentials. Front Cell Dev Biol 9: 636595, 2021.
32. Cerezo M, Guemiri R, Druillennec S, Girault I, Malka-Mahieu H, Shen S, Allard D, Martineau S, Welsch C, Agoussi S, *etal*: Translational control of tumor immune escape via the eIF4F-STAT1-PD-L1 axis in melanoma. Nat Med 24: 1877-1886, 2018.
33. Zhang J, Tan GL, Jiang M, Wang TS, Liu GH, Xiong SS and Qing X: Effects of SENP1-induced deSUMOylation of STAT1 on proliferation and invasion in nasopharyngeal carcinoma. Cell Signal 101: 110530, 2023.
34. Wong GS, Lee JS, Park YY, Klein-Szanto AJ, Waldron TJ, Cukierman E, Herlyn M, Gimotty P, Nakagawa H and Rustgi AK: Periostin cooperates with mutant p53 to mediate invasion through the induction of STAT1 signaling in the esophageal tumor microenvironment. Oncogenesis 2: e59, 2013.
35. Huang J, Ding Z, Luo Q and Xu W: Cancer cell-derived exosomes promote cell proliferation and inhibit cell apoptosis of both normal lung fibroblasts and non-small cell lung cancer cell through delivering alpha-smooth muscle actin. Am J Transl Res 11: 1711-1723, 2019.
36. Xu J, Li Y and Hu H: Effects of lycopene on ovarian cancer cell line SKOV3 in vitro: Suppressed proliferation and enhanced apoptosis. Mol Cell Probes 46: 101419, 2019.
37. Ji Y, Yu M, Qi Z, Cui D, Xin G, Wang B, Jia W and Chang L: Study on apoptosis effect of human breast cancer cell MCF-7 induced by lycorine hydrochloride via death receptor pathway. Saudi Pharm J 25: 633-637, 2017.
38. Xu G, Zhang Y, Li N, Zhang JB and Xu R: LncRNA CCHE1 in the proliferation and apoptosis of gastric cancer cells. Eur Rev Med Pharmacol Sci 22: 2631-2637, 2018.
39. Tanaka A, Zhou Y, Ogawa M, Shia J, Klimstra DS, Wang JY and Roehrl MH: STAT1 as a potential prognosis marker for poor outcomes of early stage colorectal cancer with microsatellite instability. PLoS One 15: e0229252, 2020.
40. Nivarthi H, Gordziel C, Themanns M, Kramer N, Eberl M, Rabe B, Schlederer M, Rose-John S, Knosel T, Kenner L, *et al*: The ratio of STAT1 to STAT3 expression is a determinant of colorectal cancer growth. Oncotarget 7: 51096-51106, 2016.
41. Legrier ME, Bièche I, Gaston J, Beurdeley A, Yvonnet V, Déas O, Thuleau A, Château-Joubert S, Servely JL, Vacher S, *et al*: Activation of IFN/STAT1 signalling predicts response to chemotherapy in oestrogen receptor-negative breast cancer. Br J Cancer 114: 177-187, 2016.

42. Wong GL, Manore SG, Doheny DL and Lo HW: STAT family of transcription factors in breast cancer: Pathogenesis and therapeutic opportunities and challenges. Semin Cancer Biol 86: 84-106, 2022.
43. Wudtiwai B, Makeudom A, Krisanaprakornkit S, Pothacharoen P and Kongtawelert P: Anticancer activities of hesperidin via suppression of up-regulated programmed death-ligand 1 expression in oral cancer cells. Molecules 6: 5345, 2021.
44. Okita R, Shimizu K, Nojima Y, Saisho S and Nakata M: Tofacitinib overcomes an IFNγ-induced decrease in NK cell-mediated cytotoxicity via the regulation of immune-related molecules in LC-2/ad. Thorac Cancer 12: 775-782, 2021.
45. Breitenecker K, Homolya M, Luca AC, Lang V, Trenk C, Petroczi G, Mohrherr J, Horvath J, Moritsch S, Haas L, *et al*: Down-regulation of A20 promotes immune escape of lung adenocarcinomas. Sci Transl Med 13: eabc3911, 2021.
46. Yang J, Wang X, Huang B, Liu R, Xiong H, Ye F, Zeng C, Fu X and Li L: An IFNγ/STAT1/JMJD3 axis 2021induces ZEB1 expression and promotes aggressiveness in lung adenocarcinoma. Mol Cancer Res 19: 1234-1246, 2021.
47. Hashimoto K, Nishimura S, Ito T, Kakinoki R and Akagi M: Immunohistochemical expression and clinicopathological assessment of PD-1, PD-L1, NY-ESO-1, and MAGE-A4 expression in highly aggressive soft tissue sarcomas. Eur J Histochem 66: 3393, 2022.
48. Sase S, Almad AA, Boecker CA, Guedes-Dias P, Li JJ, Takanohashi A, Patel A, McCaffrey T, Patel H, Sirdeshpande D, *et al*: TUBB4A mutations result in both glial and neuronal degeneration in an H-ABC leukodystrophy mouse model. Elife 9: e52986, 2020.
49. Sobierajska K, Ciszewski WM, Wawro ME, Wieczorek-Szukala K, Boncela J, Papiewska-Pajak I, Niewiarowska J and Kowalska MA: TUBB4B downregulation is critical for increasing migration of metastatic colon cancer cells. Cells 8: 810, 2019.
50. Vemu A, Atherton J, Spector JO Moores CA and Roll-Mecak A: Tubulin isoform composition tunes microtubule dynamics. Mol Biol Cell 28: 3564-3572, 2017.
51. Du W and Elemento O: Cancer systems biology: Embracing complexity to develop better anticancer therapeutic strategies. Oncogene 34: 3215-3225, 2015.
52. Afrang N and Honardoost M: Cell cycle regulatory markers in melanoma: New strategies in diagnosis and treatment. Med J Islam Repub Iran 33: 96, 2019.
53. Becker TM, Boyd SC, Mijatov B, Gowrishankar K, Snoyman S, Pupo GM, Scolyer RA, Mann GJ, Kefford RF, Zhang XD and Rizos H: Mutant B-RAF-Mcl-1 survival signaling depends on the STAT3 transcription factor. Oncogene 33: 1158-1166, 2014.
54. Picco ME, Castro MV, Quezada MJ, Barbero G, Villanueva MB, Fernández NB, Kim H and Lopez-Bergami P: STAT3 enhances the constitutive activity of AGC kinases in melanoma by transactivating PDK1. Cell Biosci 9: 3, 2019.
55. Regis G, Pensa S, Boselli D, Novelli F and Poli V: Ups and downs: The STAT1:STAT3 seesaw of Interferon and gp130 receptor signalling. Semin Cell Dev Biol 19: 351-359, 2008.
56. Kortylewski M, Komyod W, Kauffmann ME, Bosserhoff A, Heinrich PC and Behrmann I: Interferon-gamma-mediated growth regulation of melanoma cells: Involvement of STAT1-dependent and STAT1-independent signals. J Invest Dermatol 122: 414-422, 2004.